Journal of Hazardous Materials 189 (2011) 660–669

Contents lists available at ScienceDirect

Journal of Hazardous Materials

journal homepage: www.elsevier.com/locate/jhazmat

Use of biogenic and abiotic elemental selenium nanospheres to sequester elemental mercury released from mercury contaminated museum specimens

J.W. Fellowes[a,*], R.A.D. Pattrick[a], D.I. Green[a], A. Dent[c], J.R. Lloyd[a], C.I. Pearce[b]

[a] School of Earth, Atmospheric and Environmental Sciences, Williamson Building, University of Manchester, Oxford Road, Manchester M13 9PL, UK
[b] Pacific Northwest National Laboratory, Richland, WA, USA
[c] Diamond Light Source, Didcot, Oxfordshire, UK

ARTICLE INFO

Article history:
Received 17 September 2010
Received in revised form 14 January 2011
Accepted 17 January 2011
Available online 26 January 2011

Keywords:
Mercury contamination
Botanical collections
Geobacter sulfurreducens
Selenium nanoparticles

ABSTRACT

Mercuric chloride solutions have historically been used as pesticides to prevent bacterial, fungal and insect degradation of herbarium specimens. The University of Manchester museum herbarium contains over a million specimens from numerous collections, many preserved using $HgCl_2$ and its transformation to Hg^0_v represents a health risk to herbarium staff. Elevated mercury concentrations in work areas (~1.7 $\mu g\,m^{-3}$) are below advised safe levels (<25 $\mu g\,m^{-3}$) but up to 90 $\mu g\,m^{-3}$ mercury vapour was measured in specimen boxes, representing a risk when accessing the samples. Mercury vapour release correlated strongly with temperature. Mercury salts were observed on botanical specimens at concentrations up to 2.85 wt% (bulk); XPS, SEM–EDS and XANES suggest the presence of residual $HgCl_2$ as well as cubic HgS and HgO. Bacterially derived, amorphous nanospheres of elemental selenium effectively sequestered the mercury vapour in the specimen boxes (up to 19 wt%), and analysis demonstrated that the Hg^0_v was oxidised by the selenium to form stable HgSe on the surface of the nanospheres. Biogenic Se^0 can be used to reduce Hg^0_v in long term, slow release environments.

1. Introduction

The preservation of botanical specimens in museums across the world has traditionally proven difficult. A wide range of organic and toxic metal biocides have been used to deter the onset of decay caused by bacteria, fungi, insects and rodents; the efficiency of these treatments can be seen by the excellent state of preservation in many specimens today. The use of mercury salt solutions in the preservation of botanical specimens goes back to 1687, and continued in the UK up until the 1980s [1,2], ultimately giving way to organic pesticides including naphthalene, p-dichlorobenzene, thymol, lindane and DDT [2,3]. The preparation of mercury bearing pesticide solutions is detailed by Briggs et al. [4] and a concentration of 30 $g\,l^{-1}$ $HgCl_2$ and 30 $g\,l^{-1}$ phenol dissolved into methylated spirits was used in the Cambridge University Herbarium, UK. The low rate of sublimation of $HgCl_2$ and careful storage ensure that botanical specimens dating back hundreds of years still hold significant concentrations of Hg; as Hg^0, residual $HgCl_2$, HgS and 2HgO·HgS [2,4–10]. Amalgamation of botanical collections into large herbaria, each having undocumented preservation techniques, has lead to inhomogeneous distribution of mercury contaminated specimens within collections. Staining of sample mounting paper due to the formation of crystalline Hg phases has been used to identify the presence of Hg-bearing compounds by fluorescence using UV irradiation [2].

Health risks associated with Hg-bearing botanical samples are not confined to dermal contact with contaminated specimens; Briggs et al. [4] report the evolution of Hg^0 vapour leading to elevated local Hg concentrations of 25 $\mu g\,m^{-3}$ at the Cambridge University Herbarium. Investigations in other herbaria indicate that this problem is widespread [8,9]. The concentration of Hg^0_v is dependent on ambient temperature; Oyarzun et al. [8] show that the Hg vapour concentration in the MAF Herbarium, Spain rises from 404–727 $ng\,m^{-3}$ in late winter (23 °C) to 748–7797 $ng\,m^{-3}$ in early summer (31 °C). Oyarzun et al. [8] also show that in a well insulated herbarium such as the relatively modern MA Herbarium, Spain, Hg^0_v concentrations exceeded 40 $\mu g\,m^{-3}$.

Regulatory standards for workplace exposure limits have been summarised by Baughman [11], with guideline exposure limits varying between 25 $\mu g\,m^{-3}$ and 100 $\mu g\,m^{-3}$ Hg. It is also noted that children are much more susceptible to Hg toxicity than adults, which is of concern for public access museums.

The transformation mechanism of the relatively stable $HgCl_2$ into Hg^0 is not well understood. Oyarzun et al. [8] surmised that microbial enzymatic reduction of Hg^{2+} to Hg^0_v as part of a Hg detoxification mechanism may be responsible, and work by Roane and

* Corresponding author. Tel.: +44 161 275 3800; fax: +44 161 306 9361.
E-mail address: Jonathan.Fellowes@postgrad.manchester.ac.uk (J.W. Fellowes).

0304-3894/$ – see front matter © 2011 Elsevier B.V. All rights reserved.
doi:10.1016/j.jhazmat.2011.01.079

Snelling [12] has identified bacteria isolated from museum specimens that display a high Hg^{2+} tolerance (in excess of 10 mg l^{-1}), which may also be used as a possible remediation strategy. Complicating this process, however, is the presence of a range of other pesticides often found alongside Hg.

Briggs et al. [4] and Oyarzun et al. [8] both report that an increase in ventilation significantly drops the Hg^0_v content of the air. There are circumstances where increasing ventilation cannot be considered due to climate, expense or positioning of the herbarium within buildings, and so an alternative method for decreasing the Hg content of herbarium and museum specimens must be identified.

Johnson et al. [13] studied the capture of Hg^0_v by nanoscale sorbents, and note that elemental α-Se nanoparticles sequester Hg more efficiently than many commercially available sorbents. Se nanoparticles can be produced biogenically by bacterial reduction of soluble Se oxyanions. Se pollution, in the form of the oxyanions selenate [SeO_4^{2-}] and selenite [SeO_3^{2-}], is associated with waste materials from a broad spectrum of anthropogenic operations, including mining, agricultural, petrochemical, and industrial manufacturing operations [14]. Water-soluble forms of selenium can be microbiologically reduced to elemental selenium nanoparticles, which are less bioavailable and generally less toxic than other selenium species. The elemental selenium nanoparticles can potentially be separated from the aqueous waste stream [15]. The biologically recovered selenium nanoparticles can then be used in subsequent applications, such as the sequestration of elemental mercury released from mercury contaminated museum specimens, to offset the cost of the biological treatment [16]. This highlights how biomineralisation approaches can be applied to convert metal-containing wastes into new nanomaterials for environmental protection [17].

This research reveals the nature and extent of Hg contamination associated with museum specimens and measurement of Hg content of airspaces at the herbarium of the Manchester museum (The University of Manchester, UK), which has a botanical collection approaching a million specimens from all over the world, representing collections spanning hundreds of years. The collection is subdivided into British and European collections, as well as several smaller collections. The level of Hg contamination is inhomogeneous and poorly documented. This work also investigates the use of Se bionanominerals, which display an increased stability in comparison with their chemically synthesised counterparts [14,18,19] for the capture of Hg^0_v released from specimens within herbaria.

2. Materials and methods

All chemicals used were of analytical grade and obtained from Sigma–Aldrich (UK).

2.1. Determination of herbarium air Hg^0_v concentration

The Hg content of the herbarium air was determined using a portable mercury vapour indicator (MVI, Shawcity, Faringdon, UK). The Hg^0_v concentration of the air was determined around the central workspaces of the herbarium and in sample boxes from a number of collections. The boxes analysed were chosen at random and were analysed immediately for Hg^0_v concentration.

2.2. Sampling

The museum's herbarium specimens are mounted onto A3 sized cardboard sheets and stored in fabric lined cardboard boxes on shelves within the herbarium, as shown in Fig. 1.

Samples from the British and European collections were analysed for Hg concentration and oxidation state. Due to the irreplaceable nature of the specimens, milligram sized samples were taken and non-destructive analysis techniques (X-ray diffraction (XRD), X-ray photoelectron spectroscopy (XPS), scanning electron microscopy (SEM) coupled to energy dispersive spectroscopy (EDS) and X-ray absorption spectroscopy (XAS)) were used prior to chemical dissolution to determine bulk Hg values. Samples include leaf segments, mounting paper and plant sample debris (Table 1).

2.3. Mercury sequestration experiments

The Hg absorption capacity of dry powders of both biogenic and abiotic Se^0 was tested. Biogenic red elemental α-Se was formed by the reduction of Na_2SeO_3 by *Geobacter sulfurreducens* coupled to the oxidation of H_2. *G. sulfurreducens* (ATCC 51573) was obtained from the Geomicrobiology Laboratory (University of Manchester) collection and grown to late log phase in modified freshwater medium amended with sodium acetate and fumarate as the electron donor and acceptor, respectively [20]. Cells

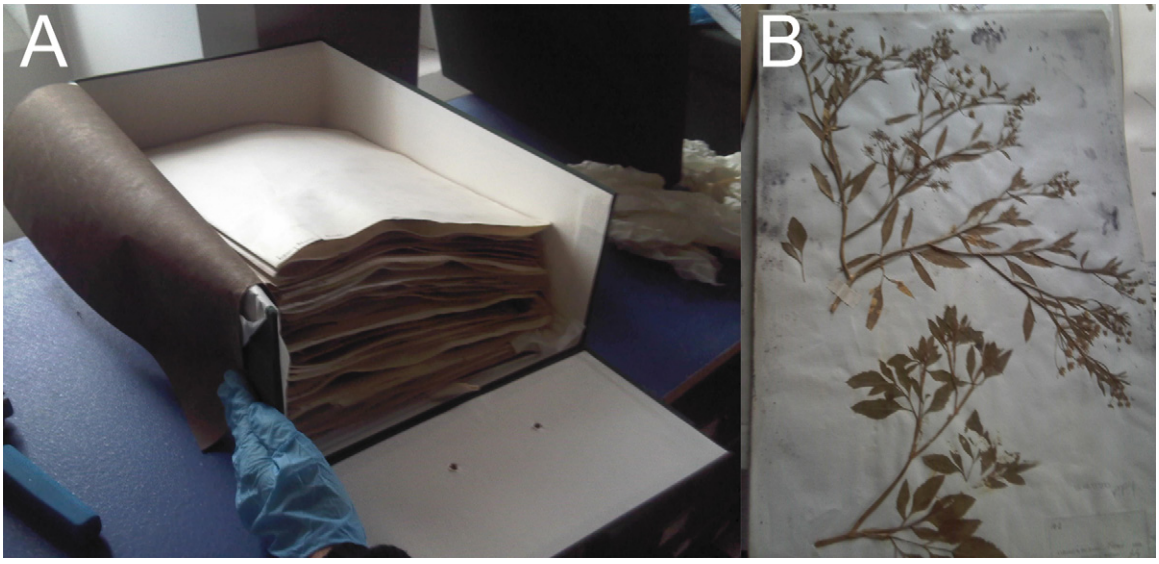

Fig. 1. Stacks of herbarium samples in containing boxes (left) and a typical herbarium specimen mounted on A3 paper with dark staining visible towards the top (right).

Table 1
Samples for analysis from the herbarium of the Manchester museum. Hg concentrations were determined by acid digestion and ICP-MS.

Sample number	Sample description	Hg concentrations (wt%)
Box 5719 *Rubus* 106		
1	Plant samples/debris, collected from crease of sample paper	0.24
2	Sample of paper with grey residue (EM322125)	N/A
3	Plant samples/debris, collected from crease of sample paper folder *Rubus incubatus* VC58 (+59 in part)	0.22
4	Material/dust collected from lining of box	2.85
Box *Scorzonera* 135.18.1		
5	Biscuit beetle, *Stegobium paniceum*	0.08
6	Plant samples/debris, collected from crease of sample paper (folder *Asteraceae* VC 58, 59, 60)	0.04
Box #6200		
7	EM35411, *Eucalyptus* leaf sample, labelled as 'poisoned'	0.08
8	Sample of paper [from 545(80)] from Hewett Cottrell Watson *Carum* sp. Folder from Azores 1842	N/A
9	Sample of stem from above	0.07

were harvested, washed and re-suspended in 20 mmol l^{-1} 3-(*N*-morpholino)propanesulfonic acid (MOPS) buffer at pH 7. Aliquots of the cell suspension were used to inoculate sterile, anaerobic solutions (final OD_{600} ~0.2) of 1 mmol l^{-1} Na_2SeO_3 in 20 mmol l^{-1} MOPS amended with 2 μmol l^{-1} of the electron shuttling compound anthraquinone-2,6-disulfonate (AQDS). The headspaces of the bottles were replaced with H_2 as an electron donor. Cultures were incubated at 30 °C and red Se^0 was precipitated. To produce abiotic Se^0, a solution containing 1 mmol l^{-1} Na_2SeO_3 and 4 mmol l^{-1} glutathione (reduced) was titrated against a 1N NaOH solution until the formation of red elemental Se was observed [13]. For the sequestration experiments, biogenic and abiotic red Se^0 suspensions (5 ml) were filtered through 0.22 μm polycarbonate micropore filters, washed with deionised H_2O (5 ml) and allowed to air dry.

2.3.1. Open system experiments

The Se^0-containing membrane filters were tested to determine the rate at which Hg^0 could be sequestered from an Hg^0-containing N_2 gas flow. The source of Hg^0_v in these experiments were solutions containing 10 ppm $HgCl_2$ and 100 ppm $SnCl_2$ [21]. N_2 was bubbled through the $HgCl_2/SnCl_2$ solutions at a varied flow rate (10–50 ml min^{-1}) and into 1 l vessels containing the Se^0 membrane filters. Effluent was passed through an acidified $KMnO_4$ solution prior to release under a fume hood [22]. The filters were exposed to the Hg^0-laden N_2 flow for 3 h and stored at −80 °C prior to acid digestion and Hg determination using ICP-MS.

Real-time determination of the effect of Se-bearing membrane filters on a metered Hg-laden gas flow was analysed via a modified Cetac M6000A Cold Vapour Atomic Absorption Spectrometer (CVAAS) mercury analyser. Modifications to this equipment involved the removal of the auto sampling stage and inline attachment of Se^0-bearing membrane filters, altering analyses from aqueous, single point Hg determination to a real-time analysis of Hg concentration in the gas phase.

2.3.2. Sealed environment experiments

The ability of the Se^0-containing membrane filters to sequester Hg^0_v was assessed under idealised laboratory conditions. Se^0 laden membrane filters were inserted into air tight 1 l jars for 1 week at constant temperature (19 °C). $HgCl_2/SnCl_2$ solutions served as the Hg^0_v source for these experiments. $HgCl_2$ concentrations ranged from 10 ppb to 10 ppm and $SnCl_2$ concentrations were kept in the ratio 1:100 Hg:Sn. After 1 week, Se^0 membrane filters were removed from the sealed jars and stored at −80 °C prior to acid digestion and Hg determination using ICP-MS.

2.3.3. In situ experiments

Biogenic Se^0-containing membrane filters were inserted into herbarium specimen boxes known to contain significant Hg^0_v concentrations (>25 μg/m^3). The samples were left for four weeks, during which the time ambient temperature rose from 19 °C to 24 °C due to weather conditions. Following collection, samples were stored at −80 °C until acid digestion for Hg determination.

2.4. Hg-species characterisation

Samples described in Table 1 and Se^0-containing membrane filters from the mercury sequestration experiments were analysed by SEM using a Philips XL30 FEG-ESEM with elemental analysis by EDAX Gemini EDS. All samples were mounted onto adhesive C-coated Al stubs to remove interference in Se determination caused by overlapping Al emission peaks. XRD of mounting paper samples (Table 1) was carried out on a Bruker D8 Advance with a Cu-Kα source. Spectra were compared to samples published by the International Centre for Diffraction Data (ICDD). XPS was carried out on sample 7 (Table 1) with a Kratos AXIS Ultra using monochromated Al Kα radiation and a wide scan pass energy of 80 eV with narrow scans recorded at 20 eV pass energy for greater chemical state resolution. The intense C 1s peak was used to normalise the energy of the spectra.

XAS was performed on samples described in Table 1 and Se^0-containing membrane filters at the Diamond Light Source, Oxfordshire, UK, on the core XAS beamline B18 where samples were analysed at the Hg L_3 absorption edge at 12.287 keV. HgS standards were used for absorption edge energy normalisation. Sample identification was via determination of inflection point difference (IPD) as described by Huggins et al. [23].

Acid digestion using *aqua regia* (1 ml) with a molar ratio 1:4 HCl:HNO_3 was used to determine the concentration of Hg in all sample materials. Excess HNO_3 was used to encourage formation of Hg^{2+} cations to decrease losses due to volatility. Samples were run on an Agilent 7500cx ICP-MS, with quoted Hg detection down of 10 ppt. A 10 ppm Au solution was run concurrently to inhibit Hg retention. To ensure complete recovery of Hg, a 1 ml HF–HCl–HNO_3 digestion (5:1:4) was used on any remaining material. The HF was neutralised using a 4 wt% solution of H_3BO_3. Owing to the necessary high dissolved solid content, these samples were analysed using a Perkin-Elmer Optima 5300 dual view ICP-AES.

3. Results and discussion

3.1. Determination of herbarium air Hg^0_v concentration

The Hg^0_v concentration of air around the work area was 1.7 μg m^{-3} at 21 °C, which did not significantly alter throughout the herbarium. These results are similar to those observed in previous studies by Oyarzun et al. [8] and Kataeva et al. [9], which

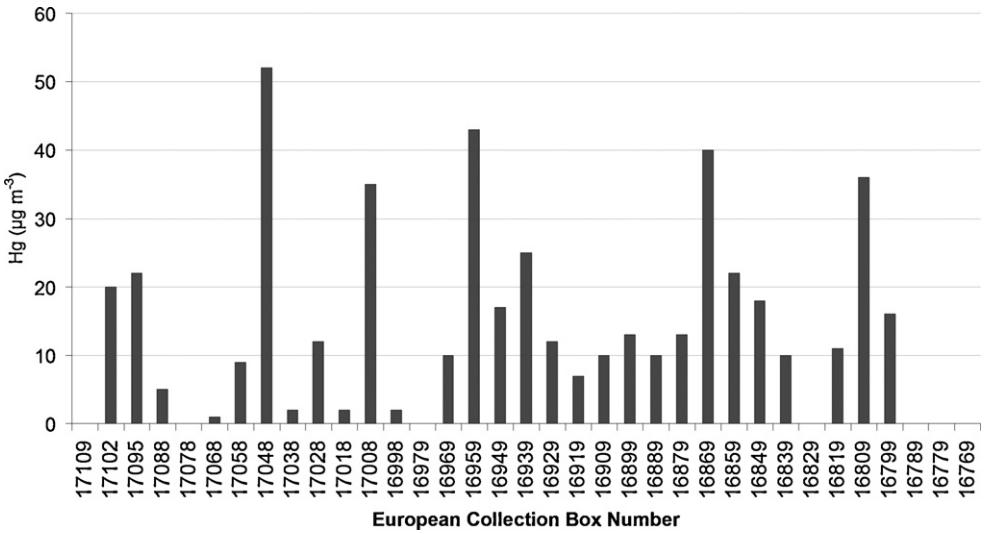

Fig. 2. Hg^0_v concentrations within herbarium specimen boxes.

recorded readings of up to 0.7 μg m^{-3} and 1.1 μg m^{-3} under similar conditions (~21–23 °C).

The Hg^0_v concentration within the specimen boxes was determined for 70 boxes from 5 collections, of which 55 came from either the British or European collections. The Hg^0_v concentrations were highly variable with the highest concentrations in the European collection with Hg^0_v ranging from below detection limits up to 52 μg m^{-3}, with 5 boxes tested recording >25 μg m^{-3} (Fig. 2). The British collection was largely free of significant Hg-contamination; however the Hg^0_v readings for the *Rubus* sp. type samples box were in excess of 40 μg m^{-3} (data not shown).

High Hg^0_v concentrations were not observed outside of the specimen boxes prior to opening, indicating that the boxes inhibit the release of Hg into the working environment.

3.2. Characterisation of museum Hg-contaminated specimens

3.2.1. Electron microscopy and X-ray diffraction

Fig. 3A shows representative SEM images of samples collected from specimen boxes containing grains of sample debris (sample 4). EDS revealed that most of the samples examined did not have significant quantities of Hg. However, analysis of one particular grain (Fig. 3B and C), showed ~1 μm particles composed of ~87 wt% Hg with the counter ions S^{2-} and Cl^-. The S component could not be quantified due to the overlap of the Hg M and S K emission lines, but the Hg wt% observed is similar to that expected from pure HgS (86 wt% as opposed to 74 wt% and 93 wt% Hg in $HgCl_2$ and HgO, respectively).

Samples of the A3 specimen mounting card (samples 2 and 8) were analysed by XRD (Fig. 4), indicating the presence of crystalline Hg phases. Sample 2 displayed peaks corresponding to unaltered $HgCl_2$ (ICDD PDF No. 00-026-0315) whilst sample 8 displayed a reflection at 26.4° 2θ, suggesting crystalline metacinnabar (ICDD PDF No. 00-006-0261). Hawks et al. [6] and Purewal et al. [2] have previously observed crystalline HgO, HgS and $HgCl_2$ phases on the mounting card.

3.2.2. XPS and XAS analysis

XPS analysis was used to identify the chemical forms of Hg present on the sample surface. Fig. 5 shows XPS spectra obtained from a *Eucalyptus* sp. leaf (sample 7) historically treated with Hg-based pesticides. XPS analysis showed that Hg was inhomogeneously distributed, with some areas falling below detection limits and others up to 1100 ppm. For the high Hg-containing areas, the

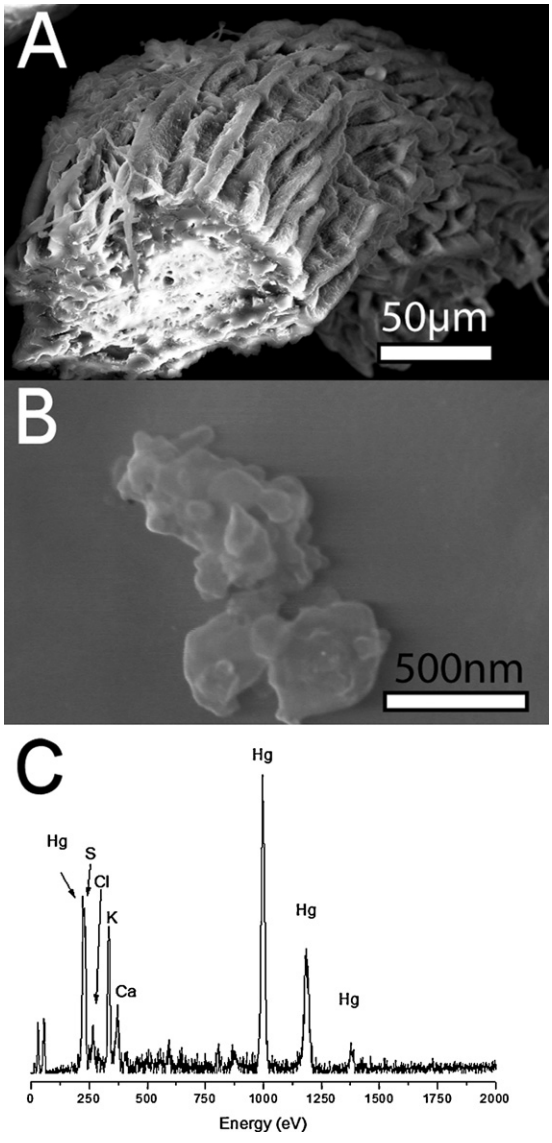

Fig. 3. SEM and EDS analysis of sample 4 (box 5719 *Rubus* sp.). (A) View of typical debris collected from within museum boxes; (B) and (C) SEM and EDS analysis showing irregular Hg-rich particles.

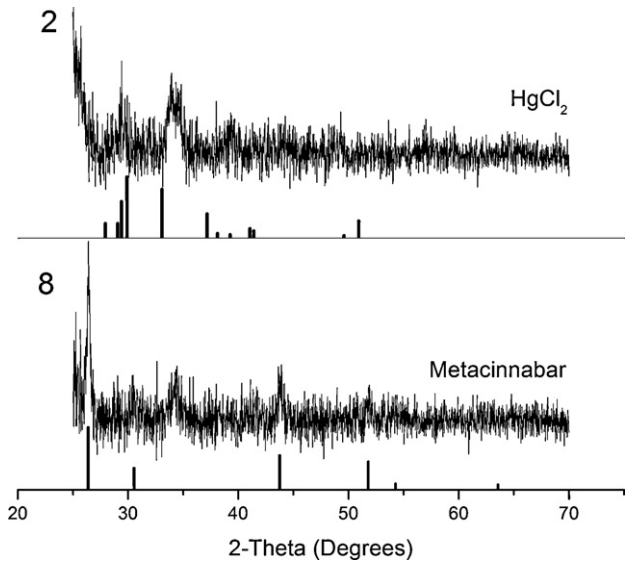

Fig. 4. XRD data from analysis of samples 2 and 8 (mounting card). (A) Indicating remnant $HgCl_2$ and (B) diffraction peaks suggesting metacinnabar.

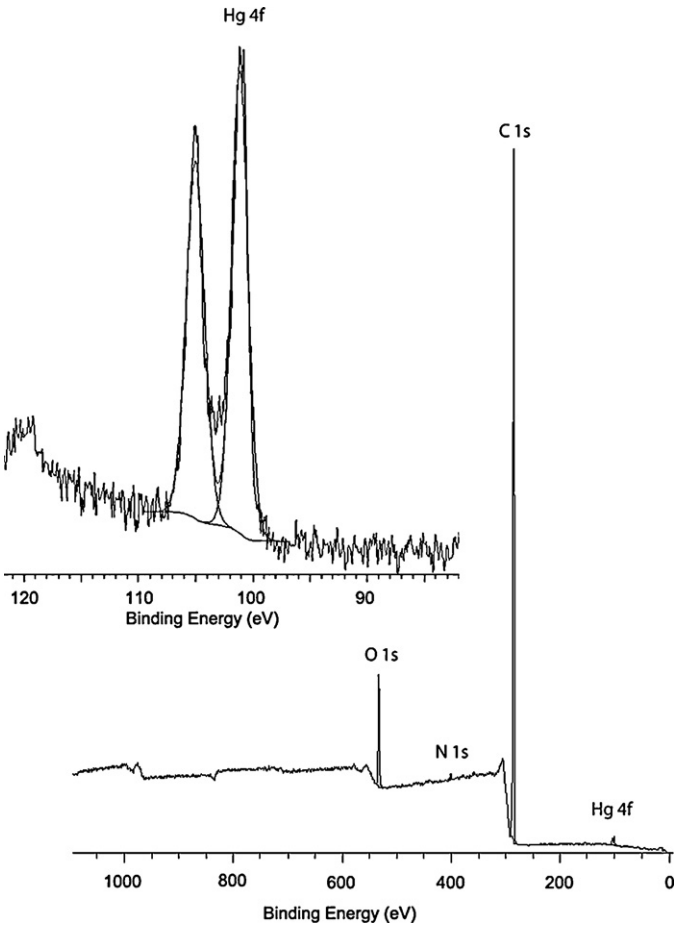

Fig. 5. XPS wide scan and inset, narrow scan spectra of *Eucalyptus* sp. leaf. Peaks correlating to Hg, C, N and O are all clearly discernable. Hg concentration determined to be ~1100 ppm.

binding energy for the Hg 4f emission was 101 eV. Comparison with published standards indicates that the Hg could be present as HgS, $HgCl_2$, HgO or as an organo-mercury compound, but precludes the presence of Hg^0 [24].

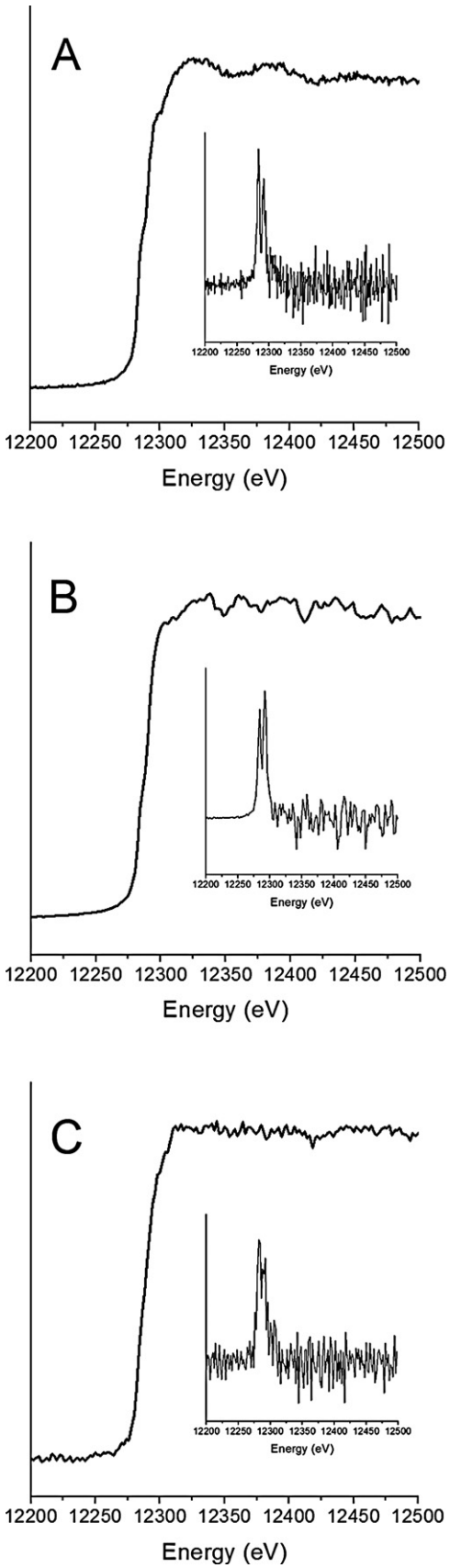

Fig. 6. XANES Hg L_3 absorption edge spectra obtained from (A) *Eucalyptus* sp. leaf; (B) box dust (sample 4) and (C) Se-laden polycarbonate membrane filter exposed to Hg^0_v. Inset: 1st derivatives of the XANES spectra.

The XANES spectrum derived from the *Eucalyptus* sp. leaf is presented in Fig. 6A, with the 1st derivative of the XANES spectrum inset. An IPD value of 7.88 eV was recorded for the first derivation, consistent with published HgS species [25]. Linear combination fitting of published HgS standards [23,25,26] suggests the XANES profile is consistent with metacinnabar, concordant with XRD findings. An IPD value of 7.89 eV was derived from the XANES analysis (Fig. 6B, inset) of the Hg-rich dust (sample 4), and is concordant with the EDS indicating the presence of a dominant HgS phase. The presence of multiple peaks in the 1st derivation of all XANES spectra obtained shows no Hg^0 is present in these samples.

3.2.3. Acid digestion of specimens in Table 1

Total extraction of Hg from the museum specimens was used to determine absolute Hg concentrations. The results of the sequential acid extractions using *aqua regia* and HF-*aqua regia* showed that Hg concentration in the specimens varied greatly (Table 1). Interestingly, the digests show that the *Eucalyptus* sp. leaf and plant stem (samples 7 and 9) do not contain significant concentrations of Hg (0.08 and 0.07 wt%). Dust and debris collected from two of the specimen wrapping sheets (samples 1 and 3) show Hg concentrations of ~0.2 wt%, but debris collected from the box containing the specimens (sample 4) had a Hg concentration of 2.85 wt%, over an order of magnitude larger. These results highlight the heterogeneity of Hg contamination within the specimens and may relate to varying pesticide coating practices. Hg contamination was found in all samples.

3.3. Mercury sequestration experiments

3.3.1. Selenium nanoparticle and filter characterisation

Selenium impregnated membrane filters were characterised prior to use in laboratory experiments by ICP-AES/-MS, SEM with EDS and particle sizing. Total acid digests showed that membrane filters were loaded with 500–600 μg of Se per filter for both abiotic and biogenic Se nanoparticles. SEM analyses of the loaded membranes prior to experimentation show smooth, spherical particles approximately 100–200 nm in diameter (Fig. 7A). EDS analyses of the Se phases (Fig. 7Di) show a dominant Se L edge peak at 1.4 eV along with smaller C and O emissions from the filter material, indicating a pure Se phase. Size distribution information was obtained (Fig. 8E) and was concordant with SEM analyses show particles ranging from 40 to 700 nm, similar to that as reported by Johnson et al. [13]. Size distribution information was used to calculate surface area assuming spherical particles; abiotic Se^0 had a surface area of 11.64 $m^2\ g^{-1}$ and biogenic Se^0 9.64 $m^2\ g^{-1}$ equating to 5.8–7.0 × 10^{-3} m^2 and 4.8–5.8 × 10^{-3} m^2 per filter, respectively.

3.3.2. Open system experiments

Biogenic Se^0-containing membrane filters were assessed using the modified CVAAS to follow the evolution of Hg^0_v from a 10 ppb Hg^{2+}/Sn^{2+} solution and to determine the effect of Se on the Hg^0_v release (Fig. 9). Evolution of Hg^0_v at a flow rate of 50 ml min^{-1} shows an initial spike corresponding to release of Hg^0_v, followed by an exponential decay over time (r^2 = 0.98). The addition of biogenic Se^0 to the inline membrane filter drastically decreased initial Hg^0_v

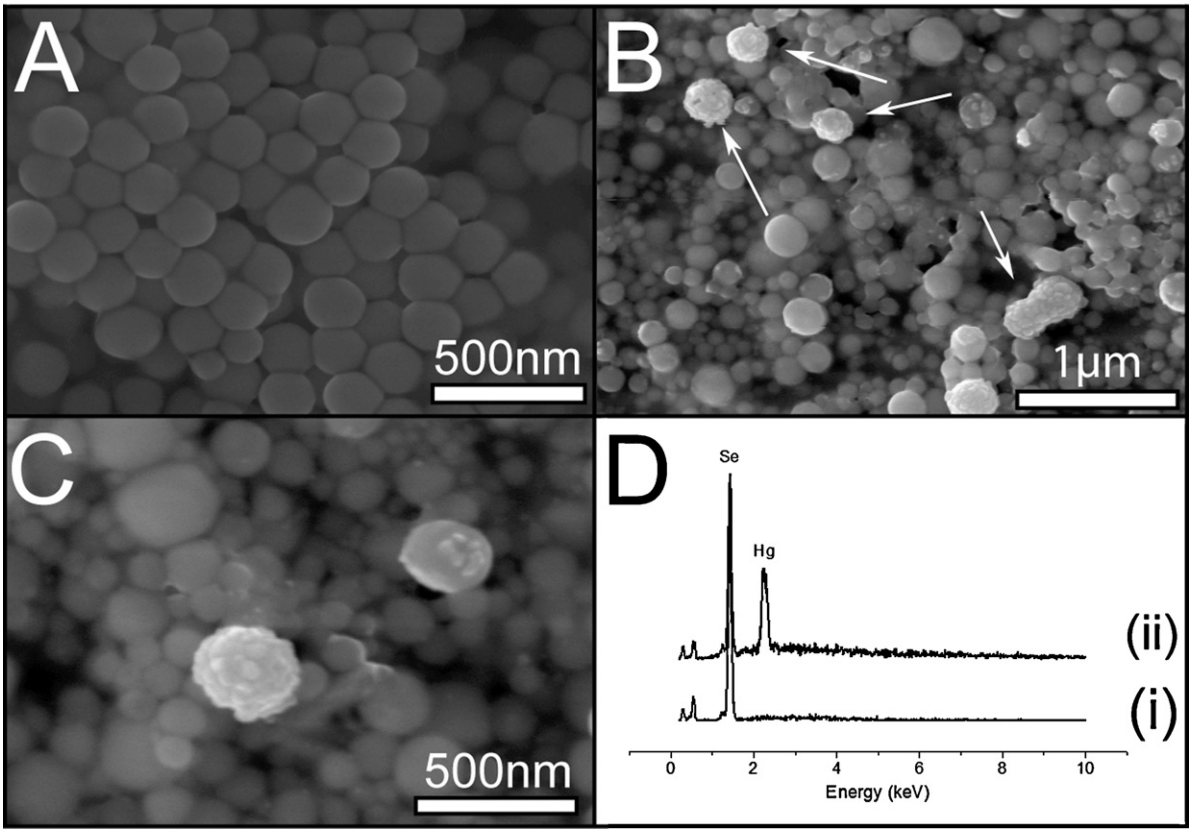

Fig. 7. (A) Initial biogenic Se^0 starting materials; (B) formation of HgSe crust following Hg^0_v exposure; (C) increased magnification view of HgSe phase; (D) EDS of biogenic Se^0 before (i) and following (ii) exposure to Hg^0_v.

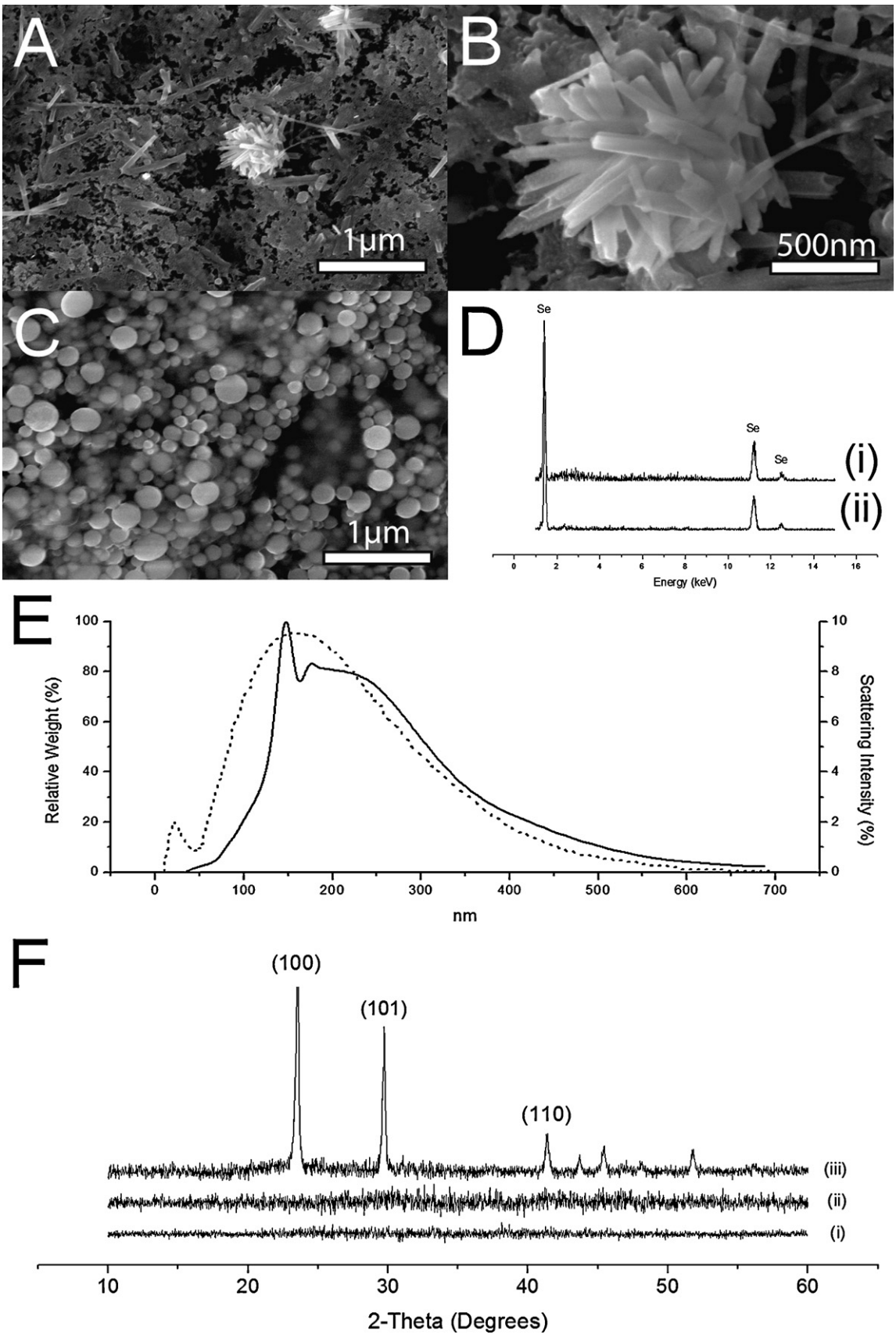

Fig. 8. Characterisation of the Se particles. (A) Crystalline Se^0 formed following crystallisation of abiotic Se^0; (B) higher magnification view of hexagonal abiotic Se^0 crystals; (C) biologically precipitated Se^0 following aging under the same conditions as (A); (D) EDS of biological (i) and abiotic (ii) Se^0 precipitates showing high purity following washing; (E) size distribution of biogenic (solid) and abiotic (dashed) Se^0 precipitates (abiotic data from Johnson et al. [13]); (F) XRD data for initial Se^0 materials (i), amorphous biogenic Se^0 after 58 days, hexagonal crystalline abiotic Se^0 after 53 days (iii).

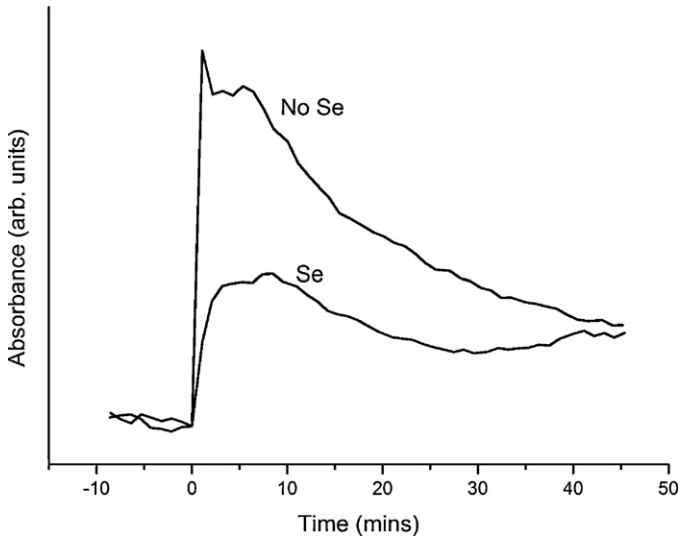

Fig. 9. CVAAS spectra for Hg concentration of gas phase with (Se) and without (No Se) Se-laden membrane filters, showing the absorption of Hg^0_v by α-Se^0 is immediate and decreases in efficiency over time.

emission (a decrease of 78% in peak intensity), and shows an overall decrease of 47% in Hg emission in the first 40 min. The extent of Hg capture decreases over time until Hg levels approach those of the system without biogenic Se^0.

Experiments comparing biogenic and abiotic Se^0-containing membrane filters at varying gas flow rates and reaction times using a 10 ppm Hg source show a strong correlation between the Hg sequestered and flow rate (Fig. 10), with a maximum Hg^0 sequestration of 3.4 mg m^{-2} for biogenic Se^0 at 10 ml min^{-1}, nearly quadruple that of Hg^0 sequestered at a flow rate of 50 ml min^{-1}. Abiotic α-Se^0 tested under the same conditions was capable of sequestering up to 7.7 mg m^{-2} of Hg^0 at 25 ml min^{-1}, more than four times that of biogenic Se^0.

3.3.3. Sealed environment experiments

Biogenic α-Se^0 was exposed to a range of $HgCl_2$ concentrations between 10 ppb and 10 ppm with $SnCl_2$ at a 1:100 Hg:Sn ratio, and an increasing trend of Hg^0_v absorption was noted (Fig. 10C), suggesting that the saturation limit of the biogenic Se^0-containing membrane filters was not reached. The maximum Hg^0 absorption of 2.2 mg m^{-2} (equivalent to 2.1% Hg by mass of Se), occurred at 10 ppm $HgCl_2$ and represented only 10% of the maximum Hg/Se mass ratio found by Johnson et al. [13]. Abiotic Se^0-containing membrane filters were able to capture >4 mg Hg^0 m^{-2}, double the capacity of biogenic Se^0.

Stock solutions of abiotic α-Se^0 were seen to change colour from red to black. XRD analysis showed the crystallisation of amorphous α-Se^0 to hexagonal Se^0 (ICDD PDF Card No. 00-006-0362), whereas biological Se^0 remained stable in suspension for over a year following synthesis (Fig. 8F). Similarly, a colour change was noted in the abiotic Se^0 impregnated membrane filters exposed to 10 ppm Hg, and subsequent SEM analyses (Fig. 8A and B) show that crystallisation of the dried Se^0 powders had occurred. EDS analysis confirmed that the crystalline Se was pure Se with no Hg, indicating recrystallisation of Se rather than neocrystallisation of an HgSe phase (Fig. 8D). Biologically precipitated α-Se^0 on the impregnated filters did not change (Fig. 8C).

Johnson et al. [13] highlighted the effect of the protein bovine serum albumin (BSA) on Se^0 powders; Hg^0 capture was hindered relative to Se^0 synthesised without BSA, despite a large increase in the available surface area. This was attributed to surface passivation by BSA, reducing the density of available reactive sites on the Se^0 particle surface. Results published by Pearce et al. [14] demonstrate the presence of surface-associated proteins on Se^0 produced by *G. sulfurreducens*, and work published by Prakash et al. [27] show that efforts to remove the biological coatings on bacterially precipitated Se^0 resulted in the formation of similar hexagonal form seen for abiotic Se^0 (Fig. 8A). Similar organic coatings have also recently been characterised by C_{60} TOF-SIMS on other complimentary bionanomaterials synthesised by *G. sulfurreducens* [28]. It is likely this surface-bound bacterially derived organic layer is increasing the

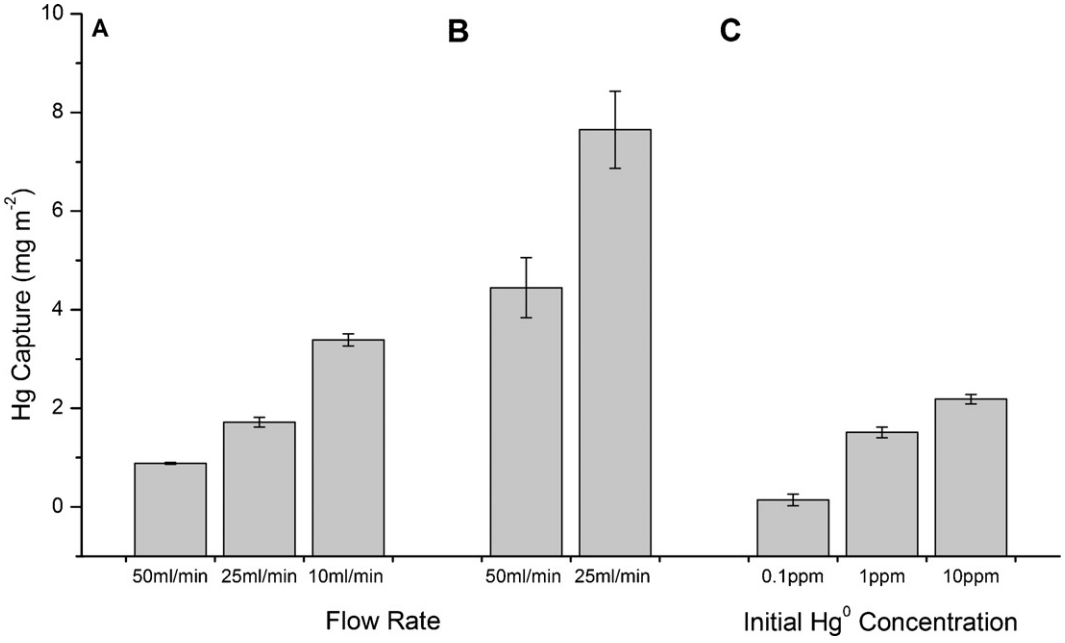

Fig. 10. The Hg content of Se-laden membrane filters following acid extraction for the biologically formed Se filter membranes (A) and abiotic Se membranes (B) under varying carrier gas flow rates. (C) The Hg concentration of biological Se membrane filters under sealed conditions.

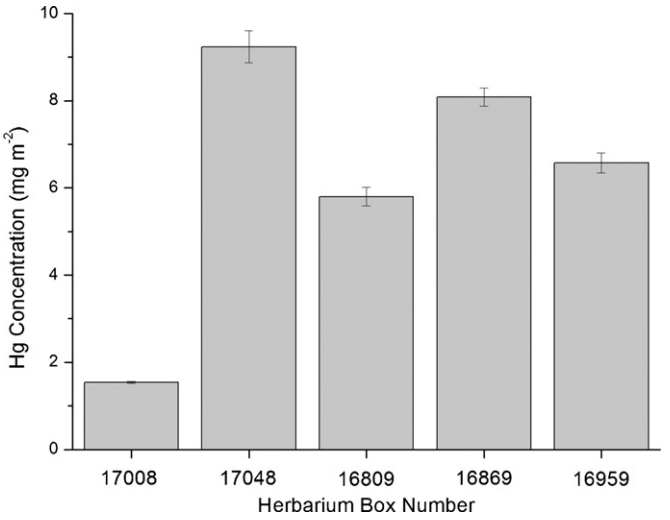

Fig. 11. Hg concentration of biogenic Se^0 filters following acid digestion and ICP analysis. Up to 9 mg m^{-2} Hg was shown to be sequestered.

stability of the Se^0 particles and passivating the surface, thus reducing Hg^0_v sequestration [14,18,27].

Despite the 50% reduction in initial Hg^0_v sequestration capacity, the long term instability of the abiotic Se^0 may render this material unsuitable for application in long term capture of Hg^0_v emission from museum specimens. Also, as bacterially precipitated Se^0 is a by-product of biological selenium treatment to remove selenate and selenite from contaminated natural waters and anthropogenic waste streams [15], the more stable bacterially precipitated Se^0 was used for further *in situ* experimentation to potentially link bioremediation strategies with production of functional bionanominerals.

3.3.4. *In situ experiments*

Biogenic Se^0-containing membrane filters were placed in five boxes of the European collection with Hg^0_v concentrations greater than 25 μg m^{-3} (Fig. 2) and left for 4 weeks. The effect of the biogenic Se^0-containing membrane filters on the concentration of Hg^0_v in the air within herbarium specimen boxes could not be determined due to the changes in ambient air temperature during the course of the *in situ* experiment; a temperature increase from 19 °C to 24 °C occurred during the 4 weeks, leading to in an increase in Hg^0_v release as previously observed by Oyarzun et al. [8]. An increase from 42 μg m^{-3} Hg^0_v to 90 μg m^{-3} in one specimen box was seen. SEM images of the biogenic Se^0 before and after exposure to Hg^0_v in the specimen boxes are shown in Fig. 7. The initial form of the α-Se^0 is as clearly defined spheres with smooth surfaces with particle sizes ranging from 35 to 680 nm (Figs. 7A and 8E). Following 4 weeks in Hg contaminated herbarium boxes, there was a morphological change of some spheres to a rough, textured surface (Fig. 7B and C). EDS spectra of remaining smooth and rough spheres showed that smooth particles contained little Hg, whereas the rough textured particles show a significant Hg concentration (Fig. 7Dii). EDS analysis showed that these particles were composed of Hg and Se (31–33% Hg by mass). As pure HgSe is ~72% Hg by mass, these results suggest that there is a significant surface coating of an HgSe phase.

Following exposure of biogenic Se^0 to Hg^0_v in the specimen boxes, a sample was analysed using XAS at the Hg L_3-edge (Fig. 6C). Linear combination fitting of the recorded XANES profiles against published standards suggests the presence of HgSe, concurrent with EDS findings. An IPD value of 7.47 eV was determined from the 1st derivation of the XANES spectra, which differs from published HgSe IPD values [23], likely as a result of the low Hg concentrations in the sample, resulting in a high signal:noise ratio (Fig. 6C, inset).

Acid digestion of the biogenic Se^0-containing membrane filters in *aqua regia* was carried out to determine total Hg concentrations (Fig. 11). All membrane filters tested showed Hg concentrations in the range 0.02–0.19 μg Hg per μg Se, corresponding to the sequestration of up to 19% Hg by mass, which is comparable to the sequestration results obtained for abiotic Se^0 by Johnson et al. [13].

The normalised concentration of Hg^0_v sequestered by the biogenic Se^0-containing membrane filters shows a linear correlation with the Hg^0_v concentration of the air within the herbarium specimen boxes.

4. Conclusion

Measurement of Hg concentrations in the Manchester museum herbarium has identified the presence of Hg^0_v both within well-sealed specimen boxes and in the air of the herbarium workspaces. The concentration of Hg^0_v in workspaces did not exceed 1.7 μg m^{-3}, which is well below the lowest advised workplace mercury exposure limit of 25 μg m^{-3}. The Hg^0_v content observed within specimen boxes was variable and sometimes very high, increasing from 43 μg m^{-3} at 19 °C to 90 μg m^{-3} at 24 °C in one box. The construction of the specimen boxes is an advantage as it prohibits the release of Hg^0_v into the workspace, but allows the build up of significant concentrations of Hg^0_v within boxes, which is released when materials are accessed. Hg-contamination of specimens is variable between collections, within collections and even within specimens stored in the same box. Hg is found on specimens predominantly as metacinnabar. However, indications of a surface coating of HgO and the presence of $HgCl_2$ suggest that the form of Hg in this system is affected by a number of factors including biological activity, oxidation and original Hg concentration. Significant quantities of Hg (2.5 wt%) were found in some specimens. Hg^0 was not found to be directly associated with the specimens, but a strong correlation between temperature and release of Hg^0_v was observed.

Biogenic α-Se^0 efficiently sequesters Hg^0_v, with a 47% initial reduction in Hg emission. Contact time between the Hg^0_v and the biogenic Se^0 nanoparticles has a significant effect on the reaction rate, with the biogenic Se^0 capturing Hg^0 more effectively at lower gas flow rates, similar to the conditions of low level, continuous Hg^0_v release expected in the sealed specimen boxes. The sequestration of the Hg^0 as a stable layer of HgSe on the surface of the nanoparticles represents a safe option to limit the release of Hg^0_v into the air. The observed absorption capacity of up to 20% Hg by mass compares favourably with that observed for abiotically synthesised α-Se^0. A major advantage of biogenic α-Se^0 over abiotic α-Se^0 is the improvement in long term stability, which offsets the initial low reaction rates with improved longer term performance. Amorphous elemental red Se nanospheres produced both biogenically and abiotically represent a promising new way to capture Hg^0_v released from Hg- contaminated herbarium specimens. The potential to use biogenic Se nanospheres, formed as a by product of biological treatment of selenium contaminated wastewater, also provides an opportunity to link bioremediation strategies with production of new nanomaterials for environmental protection.

Acknowledgements

The authors would like to thank Paul Lythgoe for ICP-MS/AES and CVAAS analysis, Cath Davies for acid digestions, Dr Paul Wincott for XPS, Dr John Waters for XRD, Dr John Charnock for advice on XAS and Dr Melanie Taylor. This research was supported by the Natural Environment Research Council (NERC), UK.

References

[1] S.H. Clark, Preservation of herbarium specimens – an archive conservators approach, Taxon 35 (1986) 675–682.
[2] V. Purewal, B. Colston, S. Rohrs, Developing a simple screening method for the identification of historic biocide residues on herbarium material in museum collections, X-ray Spectrom. 37 (2008) 137–141.
[3] P.T. Palmer, M. Martin, G. Wentworth, N. Caldararo, L. Davis, S. Kane, D. Hostler, Analysis of pesticide residues on museum objects repatriated to the Hupa Tribe of California, Environ. Sci. Technol. 37 (2003) 1083–1088.
[4] D. Briggs, P.D. Sell, M. Block, R.D. Ions, Mercury-vapor – a health-hazard in herbaria, New Phytol. 94 (1983) 453–457.
[5] J. Sirois, Analysis of mercury compounds on herbarium sheet test specimens, in: Analytical Research Laboratory Report No. 3708, Canadian Conservation Institute, Ottawa, 1998.
[6] C. Hawks, K. Makos, D. Bell, P.E. Wambach, G.E. Burroughs, An inexpensive method to test for mercury vapor in herbarium cabinets, Taxon 53 (2004) 783–790.
[7] P.J. Sirois, The analysis of museum objects for the presence of arsenic and mercury: non-destructive analysis and sample analysis, Collect. Forum 16 (2001) 65–75.
[8] R. Oyarzun, P. Higueras, J.M. Esbri, J. Pizarro, Mercury in air and plant specimens in herbaria: a pilot study at the MAF Herbarium in Madrid (Spain), Sci. Total Environ. 387 (2007) 346–352.
[9] M. Kataeva, N. Panichev, A.E. van Wyk, Monitoring mercury in two South African herbaria, Sci. Total Environ. 407 (2009) 1211–1217.
[10] J. Sirois, K. Helwig, Analysis of darkened areas on mounting papers used in historical herbarium specimens, in: Analytical Research Laboratory Report No. 3599, Canadian Conservation Institute, Ottawa, 1996.
[11] T.A. Baughman, Elemental mercury spills, Environ. Health Perspec. 114 (2006) 147–152.
[12] T.M. Roane, L.J. Snelling, Bacterial removal of mercury from museum materials: a new remediation technology? in: A.E. Charola, R.J. Koestler (Eds.), Pesticide Mitigation in Museum Collections: Science in Conservation. Proceedings from the MCI Workshop Series, Smithsonian Institution Scholarly Press, 2009, pp. 29–34.
[13] N.C. Johnson, S. Manchester, L. Sarin, Y.M. Gao, I. Kulaots, R.H. Hurt, Mercury vapor release from broken compact fluorescent lamps and in situ capture by new nanomaterial sorbents Environ. Sci. Technol. 42 (2008) 5772–5778.
[14] C. Pearce, R.A.D. Pattrick, N. Law, J.M. Charnock, V.S. Coker, J.W. Fellowes, R.S. Oremland, J.R. Lloyd, Investigating different mechanisms for biogenic selenite transformations: *Geobacter sulfurreducens*, *Shewanella oneidensis* and *Veillonella atypica*, Environ. Technol. 30 (2009) 1313–1326.
[15] M. Lenz, E.D. Van Hullebusch, G. Hommes, P.F.X. Corvini, P.N.L. Lens, Selenate removal in methanogenic and sulfate-reducing upflow anaerobic sludge bed reactors, Water Res. 42 (2008) 2184–2194.
[16] M. Lenz, P.N.L. Lens, The essential toxin: the changing perception of selenium in environmental sciences, Sci. Total Environ. 407 (2009) 3620–3633.
[17] L.E. Macaskie, I.P. Mikheenko, P. Yong, K. Deplanche, A.J. Murray, M. Paterson-Beedle, V.S. Coker, C.I. Pearce, R. Cutting, R.A.D. Pattrick, D. Vaughan, G. van der Laan, J.R. Lloyd, Today's wastes, tomorrow's materials for environmental protection, Hydrometallurgy 104 (2010) 483–487.
[18] J. Kessi, M. Ramuz, E. Wehrli, M. Spycher, R. Bachofen, Reduction of selenite and detoxification of elemental selenium by the phototrophic bacterium *Rhodospirillum rubrum*, Appl. Environ. Microbiol. 65 (1999) 4734–4740.
[19] R.S. Oremland, M.J. Herbel, J.S. Blum, S. Langley, T.J. Beveridge, P.M. Ajayan, T. Sutto, A.V. Ellis, S. Curran, Structural and spectral features of selenium nanospheres produced by se-respiring bacteria, Appl. Environ. Microbiol. 70 (2004) 52–60.
[20] J.R. Lloyd, C. Leang, A.L.H. Myerson, M.V. Coppi, S. Cuifo, B. Methe, S.J. Sandler, D.R. Lovley, Biochemical and genetic characterization of PpcA, a periplasmic c-type cytochrome in *Geobacter sulfurreducens*, J. Biochem. 369 (2003) 153–161.
[21] E. Yamada, T. Yamada, M. Sato, Determination of trace mercury in the environmental water containing iodide by using cold-vapor atomic-absorption spectrometry, Anal. Sci. 8 (1992) 863–868.
[22] L.B. Zhao, G.T. Rochelle, Hg absorption in aqueous permanganate, AIChE J. 42 (1996) 3559–3562.
[23] F.E. Huggins, N. Yap, G.P. Huffman, C.L. Senior, XAFS characterization of mercury captured from combustion gases on sorbents at low temperatures, Fuel Process. Technol. 82 (2003) 167–196.
[24] J.F. Moulder, W.F. Stickle, P.E. Sobol, K.D. Bomben, Handbook of X-ray Photoelectron Spectroscopy: A Reference Book of Standard Spectra for Identification and Interpretation of XPS Data, Perkin-Elmer Corp. (1992).
[25] F.E. Huggins, G.P. Huffman, G.E. Dunham, C.L. Senior, XAFS examination of mercury sorption on three activated carbons, Energy Fuels 13 (1999) 114–121.
[26] G.N. George, S.P. Singh, R.C. Prince, I.J. Pickering, Chemical forms of mercury and selenium in fish following digestion with simulated gastric fluid, Chem. Res. Toxicol. 21 (2008) 2106–2110.
[27] N.T. Prakash, N. Sharma, R. Prakash, K.K. Raina, J. Fellowes, C.I. Pearce, J.R. Lloyd, R.A.D. Pattrick, Aerobic microbial manufacture of nanoscale selenium: exploiting nature's bio-nanomineralization potential, Biotechnol. Lett. (2009).
[28] V.S. Coker, J.A. Bennett, N.D. Telling, T. Henkel, J.M. Charnock, G. van der Laan, R.A.D. Pattrick, C.I. Pearce, R.S. Cutting, I.J. Shannon, J. Wood, E. Arenholz, I.C. Lyon, J.R. Lloyd, Microbial engineering of nanoheterostructures: biological synthesis of a magnetically recoverable palladium nanocatalyst, ACS Nano 4 (2010) 2577–2584.